Article

# Prodrug Strategies to Improve the Solubility of HCV NS5A Inhibitor Pibrentasvir (ABT-530)

John T. Randolph, Eric A. Voight, Stephen N. Greszler, Brice Uno, James Newton, Kenneth Gleason, DeAnne Stolarik, Cecilia Van Handel, Daniel Bow, and David A. DeGoey

*J. Med. Chem.*, **Just Accepted Manuscript** • DOI: 10.1021/acs.jmedchem.0c00956 • Publication Date (Web): 03 Sep 2020

# Prodrug Strategies to Improve the Solubility of HCV NS5A Inhibitor Pibrentasvir (ABT-530)

John T. Randolph*, Eric A. Voight, Stephen N. Greszler, Brice E. Uno, James N. Newton, Kenneth M. Gleason, DeAnne Stolarik, Cecilia Van Handel, Daniel A. J. Bow, David A. DeGoey

Abbvie Incorporated, Global Pharmaceutical Research and Development

1 North Waukegan Road, North Chicago, IL 60064

KEYWORDS: hepatitis C, antiviral, NS5A, pibrentasvir, ABT-530, prodrug

**Abstract**

A research program to discover solubilizing prodrugs of HCV NS5A inhibitor pibrentasvir (PIB) identified phosphomethyl analog **2** and trimethyl-lock (TML) prodrug **9**. The prodrug moiety is attached to a benzimidazole nitrogen via an oxymethyl linkage to allow for rapid and complete release of the drug for absorption following phosphate removal by intestinal alkaline phosphatase. These prodrugs have good hydrolytic stability properties and improved solubility compared to PIB, both in aqueous buffer (pH 7) and FESSIF (pH 5). TML prodrug **9** provided superior in vivo performance, delivering high plasma concentrations of PIB in mouse, dog and monkey PK studies. The improved dissolution properties of these phosphate prodrugs give them potential to simplify drug dosage forms for PIB-containing HCV therapy.

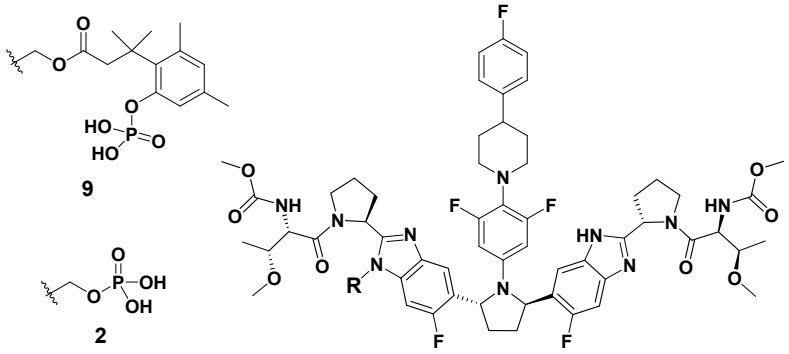

## Introduction

Pibrentasvir (ABT-530) is a second-generation HCV inhibitor that targets the NS5A protein, which is used in combination with the HCV NS3 protease inhibitor glecaprevir (ABT-493) for the treatment of HCV genotypes 1-6.[1-6] Pibrentasvir (PIB) is a single-digit picomolar inhibitor of wild-type replicons for all major HCV genotypes that maintains potency (<10-fold resistance) against variant forms of HCV that are highly resistant to other NS5A inhibitors.[7] Selection experiments in replicon cells for genotypes 1-6 found no significant resistance to PIB.[8] Treatment response in patients with chronic HCV infection is strongly associated with the presence of baseline resistance-associated substitutions (RASs) to HCV direct-acting antivirals (DAAs). This is particularly true in the case of NS5A inhibitor-containing regimens, since NS5A inhibitor-resistant viruses have better fitness and persist much longer than viruses that are resistant to NS5B and NS3/4a inhibitors. The presence of baseline RASs had minimal impact on SVR rates for GT 1-6 HCV patients treated with glecaprevir/pibrentasvir (G/P) in registration trials.[9] This is consistent with findings that PIB treatment-emergent NS5A variants have multiple resistance-conferring mutations (no single-mutation resistant variants observed), and replicons engineered to contain the PIB-resistant mutations have poor replicative fitness.[10]

Mavyret is a fixed dose combination of 300 mg glecaprevir (GLE) and 120 mg PIB that is administered as three pills, once a day, with food.[11] A key determinant in the daily dose of PIB is the effect of the intestinal P-gp transporter on drug absorption. Human PK studies found a greater than linear increase in plasma drug concentrations with oral doses up to 120 mg, which is the dose required to saturate transporter effects.[12] Furthermore, co-dosing with 300 mg of GLE, a P-gp inhibitor, boosts human plasma drug concentrations of PIB by 3-fold.[13] Each one-gram Mavyret capsule contains 100 mg of GLE and 40 mg of PIB, as well as 860 mg of excipients to help stabilize the drugs in the amorphous form, improving solubility and drug delivery. While both GLE and PIB are large drug molecules with physicochemical properties that present challenges for dosing, PIB presents the far greater challenge, as evidenced by the comparison of properties in Figure 1. PIB has a much higher MW and LogD and is essentially insoluble in water at neutral pH. PIB is also much more highly bound to human plasma proteins and has poor in

vitro permeability, with no measurable passive diffusion in PAMPA and apparent permeability ($P_{app}$) <1 X 10 $^{6}$ cm/s in canine kidney epithelial (MDCK) cells.

Figure 1. Physicochemical properties of glecaprevir and pibrentasvir.

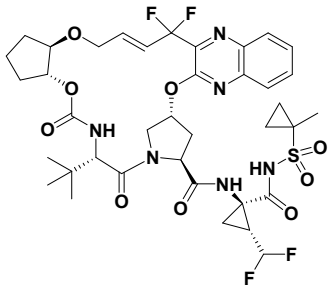

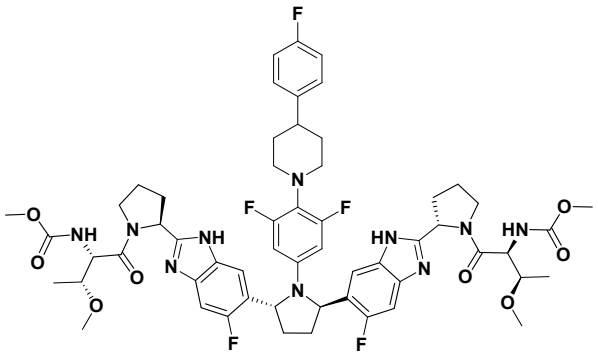

| **Glecaprevir (GLE)** | **Pibrentasvir (PIB)** |
|---|---|
| MW = 839 | MW = 1113 |
| LogD = 2.5 | LogD = 5.7 |
| Aq sol. (pH 7) = 0.3 mg/mL | Aq sol. (pH 7) < 0.0001 mg/mL |
| Aq sol. (pH 2) < 0.1 mg/mL | Aq sol. (pH 1) = 0.42 mg/mL |
| FeSSIF sol. (pH 5) = 0.04 mg/mL | FeSSIF sol. (pH 5) = 0.17 mg/mL |
| PAMPA = 5.2 x $10^{-6}$ cm/s | PAMPA = 0.0 x $10^{-6}$ cm/s |
| MDCK = 1.4 x $10^{-6}$ cm/s | MDCK < 1 x $10^{-6}$ cm/s |
| Human PPB = 97.5% | Human PPB > 99.9% |

PIB is the largest drug molecule approved for oral administration since cyclosporine A received FDA approval in 1983, and as such PIB presents unique and perhaps unprecedented problems for achieving a convenient oral dosing formulation.[14-16] Indeed, the poor solubility properties of PIB necessitate a high excipient/drug ratio to provide good drug absorption, and this is the primary reason that the G/P drug combination is delivered in a three-pill, once-daily regimen. With the goal of providing a treatment option for HCV patients with a reduced pill burden, we investigated solubilizing prodrugs of PIB that could enable a single pill G/P formulation with bioequivalence to Mavyret. Our studies primarily focused on PIB prodrug designs that employed a phosphate solubilizing group. Phosphates provide good water solubility and chemical stability properties, and a variety of phosphate prodrugs are described in the literature that are designed to rapidly bioconvert to release the parent drug by the action of phosphatases that are abundant in the brush border of enterocytes.[17] Phosphate prodrugs

have been successfully applied in research to identify new antiretroviral agents that reduce pill burden by improving dissolution of HIV protease inhibitors and lowering the excipient/drug ratio.[18-21]

Figure 2. Design strategies for solubilizing prodrugs of PIB.

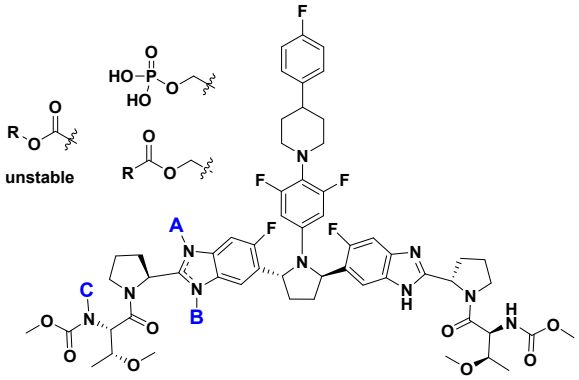


PIB presents several unique chemistry challenges to identify soluble prodrugs that efficiently deliver the drug molecule *in vivo* and have stability properties suitable for development. Not the least of these is the absence of a hydroxyl or amine group on the drug molecule to serve as a convenient handle for prodrug substitution. Available groups for attaching a prodrug moiety include the benzimidazole nitrogen atoms and the carbamate nitrogens at the dipeptide endcap termini. Success was highly dependent on identifying linkers (promoieties) that would provide good hydrolytic stability while also being rapidly cleaved by enzymes in the intestine to release PIB at the site of absorption. Suitable linkers were limited to alkyl substituents due to the hydrolytic instability of acylimidazole and imide functionalities (ie., carbamate linking groups). An oxymethyl linking group provided a viable strategy for introducing solubilizing groups on the imidazole rings at positions A or B. This approach provided prodrugs with good stability properties that efficiently deliver PIB following enzymatic removal of the solubilizing group due to hydrolytic instability of the hydroxymethyl intermediate. The simplest application of this strategy was to introduce a phosphomethyl substituent at position A or B, and this was the initial focus of the medicinal chemistry team. Alternatively, a solubilizing group could be introduced via an ester linkage on the oxymethyl substituent at positions A or B. These strategies could not be applied to attach prodrugs at

position C, since the hydroxymethyl intermediate was found to be hydrolytically stable, thus undermining efficient drug release.

Because the benzimidazole nitrogen atoms are not chemically equivalent, introducing solubilizing groups at positions A and B resulted in the formation of mixtures of isomeric prodrugs that had to be separated. Solubility and stability properties of the individual benzimidazole-linked prodrug isomers were not equivalent. Finally, the $C_2$-symmetrical structure of PIB presented challenges in minimizing the production of bis-substituted analogs having solubilizing groups on both benzimidazoles. A single solubilizing prodrug group was preferred to avoid problems with efficient drug release that could result from having two prodrug groups. While prodrugging position C would potentially simplify the chemoselectivity problem (two identical carbamate groups), modifying the terminal carbamate presented different synthetic challenges, and limited efforts will not be described here.

**Chemistry**

Phosphomethyl prodrugs were synthesized by reacting PIB with sodium hydride in anhydrous DMF at 0 $^{o}$C, followed by the addition of 1.0 equivalents of di-tert-butyl (chloromethyl)phosphate (Scheme 1). The crude alkylation product was reacted with HCl in dioxane, and the product mixture was separated by C18 HPLC to give the mono-phosphomethyl products **1** and **2** in >30% overall yield. Bis-phosphomethyl prodrugs were prepared in a similar manner by reacting with 3 equivalents of the chloromethylphosphate alkylating reagent, and were obtained in a 1:2:1 ratio of “up,up”, “up,down”, and “down,down” isomers by HPLC purification.

Chloromethyl ester alkylating reagents were used to prepare prodrugs having oxymethyl ester linkages to the benzimidazole group. The chemistry to install the prodrug could be directed to a single benzimidazole group by blocking the other benzimidazole with a Boc protecting group. Mono-Boc analog **3** (Scheme 1) could be obtained in approximately 50% yield by reacting PIB with 0.8 equivalents of di-*tert*-butyl decarbonate and catalytic DMAP in tetrahydrofuran, followed by separation of the product mixture by column chromatography on silica gel. This process favored formation of the “down” Boc isomer depicted in the scheme,

but both isomers were present in the product. Chloromethyl ester reagents, prepared from the corresponding carboxylic acids by reaction with chloromethyl chlorosulfate under phase-transfer conditions, were reacted with **3** to give the desired mono-alkylated benzimidazole products as a mixture that favored the "up" isomer, usually by at least 3 to 1. This approach allowed for the use of excess alkylating reagent to drive the reaction to completion. Removal of the Boc protecting group with TFA gave prodrugs **4**, which were separated from the minor "down" isomer by HPLC.

**Scheme 1**

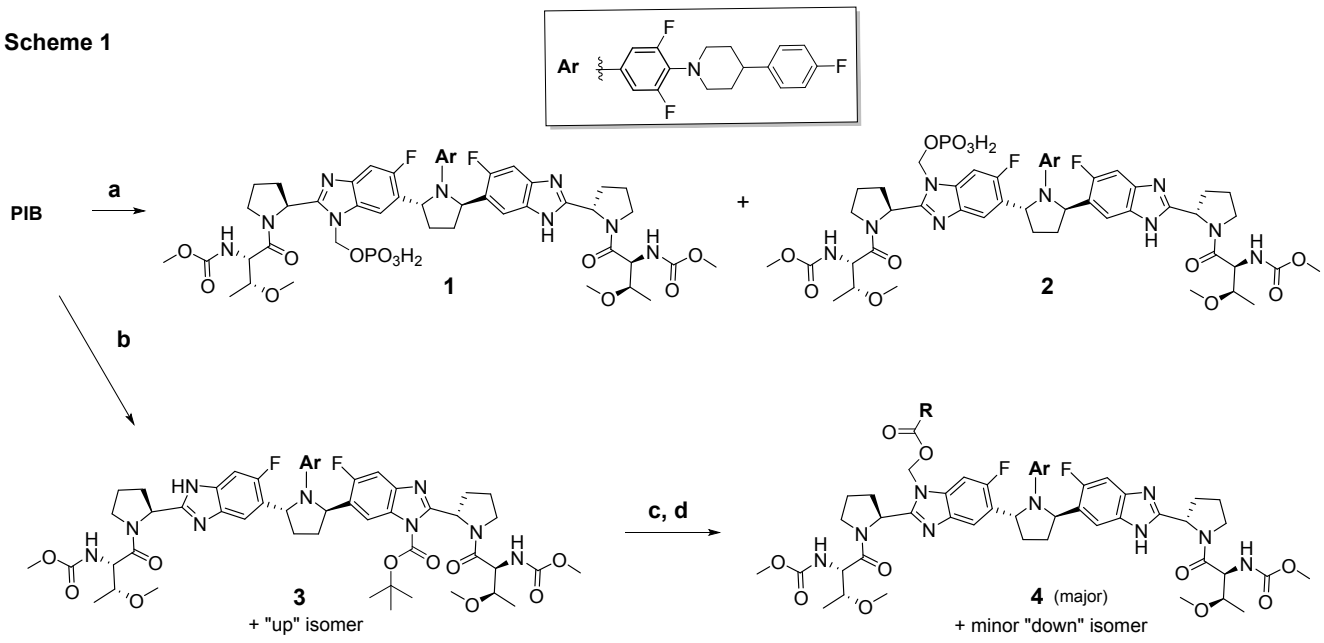


**Reagent conditions:** **a.** *i.* sodium hydride, di-*tert*-butyl (chloromethyl)phosphate, DMF, 0 $^{o}$C; *ii.* 4N HCl in dioxane; **b.** di-*tert*-butyl dicarbonate, DMAP, THF; **c.** **R**$CO_2CH_2Cl$, $Cs_2CO_3$, DMF; **d.** TFA, $CH_2Cl_2$.

An alternative approach to prodrugs **4** was to avoid Boc intermediate **3** and alkylate PIB with the chloromethyl ester reagents. This approach required the use of less than 1 equivalent of alkylating reagent to provide the desired mono-alkylated benzimidazole product as the major reaction component. Purification of the final products required removal of minor bis-alkylated products and unreacted PIB by HPLC. While the Boc-protection approach via intermediate **3** eliminated bis-alkylation products and simplified the final HPLC purification, the overall yield of prodrug was similar due to the inefficient protection step (conversion of PIB to **3**). This is illustrated in Scheme 2, which shows a synthesis of prodrugs using both approaches. The *tert*-

butyl phosphate derivative of methyl 4-hydroxy-phenylacetate was prepared using the 2-step sequence of phosphite formation followed by peroxide oxidation. Ester hydrolysis was followed by chloromethylation using phase-transfer conditions to give chloromethyl ester **5**. This reagent was used to alkylate Boc-protected PIB intermediate **3** using cesium carbonate as the base to give a 51% yield of isomeric products that favored the "up" isomer (substitution at position A in Figure 2). Removal of the t-butyl and Boc protecting groups using TFA in dichloromethane, followed by HPLC purification to remove the minor "down" isomer provided prodrug **6** in 31% overall yield (based on consumed **3**). In another example, carboxylic acid **7**, prepared using the published procedure,[22] was converted to the chloromethyl ester alkylating reagent **8**, which reacted with PIB using potassium *tert*-butoxide as the base to give a 39% yield of mono-alkylated isomeric products that strongly favored the "up" isomer (position A in Figure 2). Debenzylation and HPLC purification provided prodrug **9** in 24% overall yield (based on consumed PIB).

**Scheme 2**

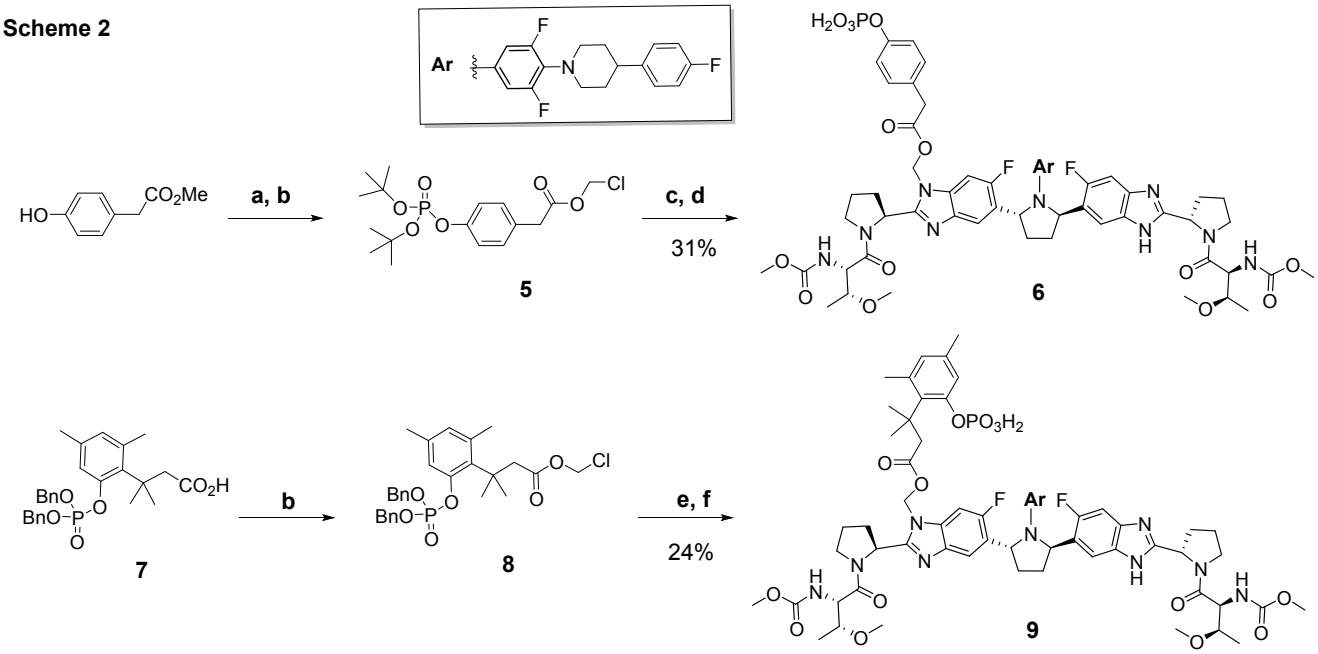


**Reagent conditions:** **a.** *i.* 1*H*-tetrazole, di-*tert*-butyl diisopropylphosphoramidite, DMA, *ii.* 50% aq. $H_2O_2$, *iii.* LiOH, aq. THF; **b.** $NaHCO_3$, chloromethyl chlorosulfate, tetrabutylammonium hydrogen sulfate, water, $CH_2Cl_2$; **c.** $Cs_2CO_3$, **3**, DMF; **d.** TFA, $CH_2Cl_2$; **e.** potassium *tert*-butoxide, PIB, DMF; f. $Pd(OH)_2$, $H_2$, THF.

## Results and Discussion

Table 1. Properties of phosphomethyl PIB prodrugs.

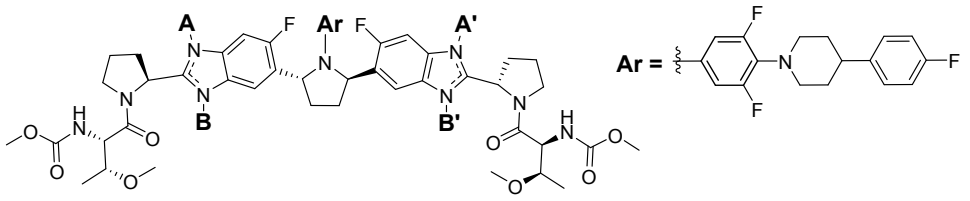


| Compd ID | Prodrug structure | | | | | Aq. Solubility (μg/mL) | | Stability[a] | |
|---|---|---|---|---|---|---|---|---|---|
| | | A | B | A' | B' | pH 1 | pH 7.4 | pH 1 | pH 7.4 |
| PIB | | H | | H | | 422 | <0.1 | | |
| 1 | 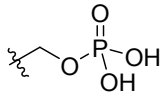 | | X | H | | >4000 | >4000 | 100% | 100% |
| 2 | | X | | H | | 37.3 | 6.4 | 100% | 100% |
| 10 | | X | | X | | 134.7 | 122.8 | 100% | |
| 11 | | | X | | X | 566.6 | >1000 | | |
| 12 | | X | | | X | >1000 | >1000 | | |

| Compd ID | dog PK (40 mg p.o.)[b] | | | | mouse PK (3 mg/kg p.o.)[b] | | | |
|---|---|---|---|---|---|---|---|---|
| | PIB | | Prodrug | | PIB | | Prodrug | |
| | $C_{max}$ | AUC | $C_{max}$ | AUC | $C_{max}$ | AUC | $C_{max}$ | AUC |
| PIB[c] | 239 | 2730 | - | - | - | - | - | - |
| PIB | 339 | 3860 | - | - | 280 | 5170 | - | - |
| 1 | 152 | 1470 | 20 | 93 | 17 | 278 | 2.2 | 12.6 |
| 2 | 55 | 429 | 0 | 0 | 141 | 2660 | 0 | 0 |
| 10 | 40 | 355 | | | 396 | 6070 | | |
| 11 | 66 | 611 | | | 20 | 353 | | |
| 12 | 275 | 2580 | | | 28 | 477 | | |

[a] Percent prodrug remaining after 24 h at 37 °C in 0.1 N aq HCl (pH 1) or phosphate buffer (pH 7.4); [b] Doses adjusted for MW of the prodrug to give an equivalent dose to PIB; [c] 40 mg PIB phase 2 tablet; Vehicle = 1:99 (v/v) DMSO:0.2% copovidone in FASSIF; $C_{max}$ (ng/mL); AUC (ng·h/mL).

Phosphomethyl prodrugs (Table 1) had good hydrolytic stability, with no degradation observed by HPLC following 24-hour incubation at 37 °C in either 0.1 N aq HCl or neutral pH phosphate buffer. Solubility and PK properties differed based on the position of the prodrug substituent. Prodrug **1**, which has the phosphomethyl substituent in position B, was much

more soluble than prodrug **2**, which is substituted in position A. The reason for the large difference in solubility is not understood but may be due to a difference in structural conformation resulting in a disparity in solvent access for the phosphate groups. The role played by the benzo-ring substituents (fluorine and pyrrolidine) on the relative solubility of these 2 regioisomeric prodrugs is not known. Solubility of the 3 isomeric bis-phosphomethyl prodrugs **10**, **11**, and **12** was not improved in comparison to prodrug **1**.

The ability of phosphomethyl prodrugs to release the drug PIB was assessed in PK studies in dog and mouse. Oral doses were adjusted for MW of the prodrug to deliver an equivalent dose of PIB. Dog studies provided a comparison between dosing the prodrug and dosing the 40 mg tablet (amorphous drug in a polymer support) that was used in Phase 2 clinical studies (crushed to facilitate dosing in dog). The more soluble prodrug **1** gave better plasma drug concentrations in dog than prodrug **2**, but plasma drug concentrations in mouse were much better for prodrug **2**. Low plasma concentrations of the prodrug were observed in both dog and mouse for prodrug **1**, but not for prodrug **2**. The bis-phosphomethyl prodrugs also showed species variability in drug delivery, with the unsymmetrically substituted prodrug **12** giving the best performance in dog and prodrug **10** giving the best performance in mouse. All phosphomethyl prodrugs gave poor PK results in at least one species in comparison to dosing with PIB. Very importantly, PK results in mouse were not predictive of results in dog, indicating that screening prodrugs in mouse would not be a dependable strategy.

The observed variability and suboptimal performance in PK studies raised concerns that simple phosphomethyl prodrug designs could be poor substrates for alkaline phosphatase enzymes, resulting in inefficient drug release in the gut. Thus, alternative prodrug designs having a variety of promoiety linking groups between the solubilizing group and the large drug molecule were explored (Table 2). Carbamate-linked phosphate prodrug **13** showed good solubility in neutral pH phosphate buffer, and much improved solubility in fed-state simulated intestinal fluid (FESSIF) in comparison to PIB. Not surprisingly, the acylimidazole linkage resulted in some loss in solubility at low pH. It was also not surprising that acyl-linked prodrug **13** had poor hydrolytic stability, with less than 20% prodrug remaining after 3 hours in neutral phosphate buffer. The poor hydrolytic stability of prodrug **13** was also observed with a few

other carbamate-linked designs that were investigated but not included in Table 2, and the combined stability data for these prodrugs indicated that prodrug attachment to the benzimidazole would require an alkyl linkage to provide hydrolytic stability suitable for development.

Valine ester prodrugs have been extensively applied in antiviral and anticancer drug research due to their ability to improve absorption of nucleoside analogs through active uptake by peptide transporters.[23-25] Our investigation of valine ester prodrugs of PIB was based in part on the possibility for solubility improvement by simple structural desymmetrization. Unfortunately, valine ester prodrugs **14** and **15** had poor hydrolytic stability and did not improve solubility in phosphate buffer in comparison to PIB. Although prodrug **14** provided good plasma concentrations of PIB in PK studies, unwanted concentrations of the prodrug were also observed in dog plasma. Bis-valine ester prodrugs having a valine ester substituent attached to both benzimidazole groups were also investigated, but bis-valine ester prodrugs were found to have solubility and hydrolytic stability properties that were no better than mono-ester prodrugs **14** and **15**.

Prodrugs with better hydrolytic stability were achieved by acylating the valine ester beta-amino group. Phosphoglycolate **16**, fumarate **17**, and phosphomethylcarbamates **18** and **19,** were stable at pH 1. However, the half-life in phosphate buffer at 37 $^{o}$C was < 24 hours for these valine ester-linked prodrugs. Phosphate prodrugs **16** and **18** had surprisingly poor solubility at neutral pH, providing little or no improvement relative to PIB. The excellent solubility for prodrug **19** in comparison to **18** again demonstrated the superior solubility properties for prodrugs having a solubilizing substituent in position B on the benzimidazole ring. Unfortunately, the chemistry to make these oxymethyl ester prodrugs was selective for the A-substituent regioisomer (product ratio ~5:1 A:B under standard alkylation conditions using cesium carbonate and the Boc-protected valine chloromethylester alkylating agent). Both phosphomethylcarbamate prodrugs **18** and **19** gave high plasma concentrations of PIB in mouse PK studies. However, **18** performed poorly in dog, and **19** was not tested in dog because of its undesirable hydrolytic stability profile, as well as the inefficient synthetic route.

Prodrugs having carboxylic acid solubilizing groups were also investigated, such as benzoic acid prodrug **20**, which had poor solubility properties. Prodrug **20** was tested as a mixture of regioisomers due to difficulty isolating the individual prodrug isomers in pure form. Mouse PK found that **20** provided low concentrations of PIB and significant concentrations of the prodrug in plasma samples, indicating undesired absorption of carboxylic acid prodrugs (also observed for fumaric acid prodrug **17**). The phosphate-substituted phenylacetate prodrug **6** was more soluble than benzoic acid **20** in neutral pH phosphate buffer and provided good plasma concentrations of PIB in the PK studies. Benzoate-linked prodrugs **21** and **22** had better hydrolytic stability and improved solubility compared to phenylacetate-linked prodrug **6**, but prodrugs **21** and **22** did not perform well in PK studies.

Table 2. Properties of ester-linked oxymethyl benzimidazole PIB prodrugs.

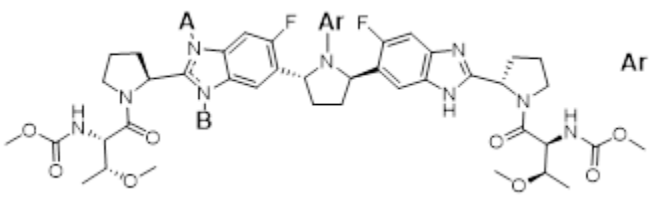


| Compd ID | Prodrug structure | A | B | Solubility (μg/mL) pH 1 | pH 7.4 | FeSSIF | Stability[a] pH 1 | pH 7.4 | Plasma PIB concentrations[b] Mouse $C_{max}$ | Mouse AUC (PD) | Dog $C_{max}$ | Dog AUC (PD) |
|---|---|---|---|---|---|---|---|---|---|---|---|---|
| PIB | | H | | 422 | <0.1 | 169 | | | 408 | 6720 | 339 | 3860 |
| 13 | 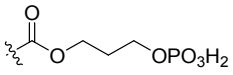 | X | | 23 | 631 | >1000 | 54% | <1% | 26 | 456 (0) | 196 | 2140 (0) |
| 14 | 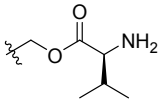 | X | | >1000 | <0.1 | >1000 | 78% | 5% | 129[c] | 2340 (0)[c] | 379 | 3940 (568) |
| 15 | | | X | >1000 | <0.2 | | | | | | | |
| 16 | 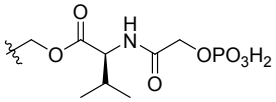 | X | | 186 | 0.7 | | 97% | 31% | 216[c] | 3710 (0)[c] | 112 | 1210 (0) |
| 17 | 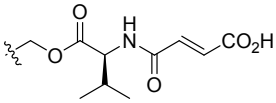 | X | | 203 | <0.2 | 542 | 97% | 67% | 15 | 231 (354) | 0 | 0 (0) |
| 18 | 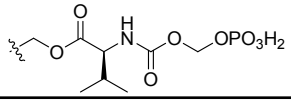 | X | | 114 | <0.1 | >1000 | 95% | 38% | 498 | 8840 (0) | 16 | 122 (0) |
| 19 | | | X | 271 | >1000 | >1000 | 95% | 28% | 513 | 8930 (0) | | |
| 20 | 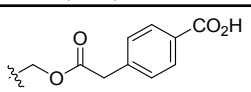 | X | X | 232 | <0.2 | 122 | 77% | 59% | 59 | 1100 (413) | | |
| 6 | 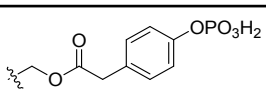 | X | | 45 | 135 | >1000 | 74% | 71% | 905 | 16100 (0) | 155 | 1920 (0) |
| 21 | 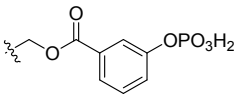 | X | | 397 | 827 | >1000 | 96% | 100% | 96 | 1510 (0) | 0 | 0 (0) |
| 22 | | | X | >1000 | >1000 | | 91% | 100% | 46 | 819 (0) | | |
| 23 | 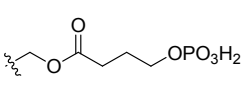 | X | | 146 | 49 | >1000 | 82% | 76% | 336 | 5570 (0) | 462 | 4510 (0) |
| 24 | | | X | 609 | 874 | >1000 | 76% | 80% | 784 | 12600 (0) | | |
| 25 | 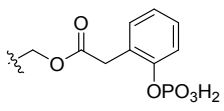 | X | | 2 | <0.2 | >1000 | 15% | 28% | 584 | 9560 (0) | 288 | 2940 (0) |

| | | | | | | | | | | | | |
|---|---|---|---|---|---|---|---|---|---|---|---|---|
| **26** | 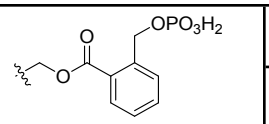 | **X** | | **99** | **<0.2** | **>1000** | **99%** | **89%** | **622** | **10700 (0)** | **115** | **1150 (0)** |
| **27** | | | **X** | **543** | **92** | **>1000** | **98%** | **84%** | **132** | **2420 (0)** | | |
| **28** | 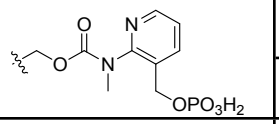 | **X** | | **>1000** | **>1000** | **>1000** | **92%** | **92%** | **380** | **6490 (0)** | **297** | **3020 (0)** |
| **29** | | | **X** | **>1000** | **>1000** | **>1000** | **92%** | **90%** | **567** | **9750 (0)** | | |
| **9** | 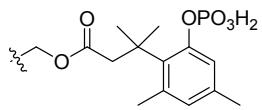 | **X** | | **572** | **0.5** | **794** | **87%** | **100%** | **1210** | **20600 (0)** | **249** | **3210 (0)** |

[a] Percent prodrug remaining after 24 h at 37 °C in 0.1 N aq HCl (pH 1) or phosphate buffer (pH 7.4); [b] Prodrugs dosed p.o. in dog (equiv. to 40 mg PIB) or mouse (equiv. to 6 mg/kg PIB) in 0.2% HPMC (doses adjusted for MW of the prodrug); [c] Prodrug **14** and **16** mouse dose equiv. to 3 mg/kg PIB; AUC (ng·h/mL); prodrug (PD) AUC in parenthesis.

A variety of self-immolative prodrugs were investigated that were designed to release PIB through an intramolecular lactonization following dephosphorylation. A self-releasing mechanism was expected to contribute to better PK performance across species, since drug-release would not be dependent on esterase expression levels. In general, self-immolative prodrugs that were investigated all provided good plasma PIB concentrations in both mouse and dog PK studies. Phosphobutyrate prodrugs **23** and **24** provided further evidence for the differences in solubility properties that favor prodrug substituents on position B of the benzimidazole (Figure 2). Phenylacetate-linked ortho-phosphate prodrug **25** had poor hydrolytic stability, whereas benzoate-linked ortho-phosphomethyl prodrugs **26** and **27** had better stability and improved solubility. However, prodrug **26** had poor solubility at neutral pH, and the more soluble isomer **27** provided only modest plasma concentrations of PIB in a mouse PK study. Phosphomethylpyridyl carbamate prodrugs **28** and **29**, which employ phosphate versions of a prodrug design used in a marketed antifungal agent,[26] had excellent solubility and hydrolytic stability properties and performed well in PK studies. Unlike other prodrugs where both benzimidazole regioisomers were tested, these pyridylcarbamate-linked prodrugs had excellent solubility properties regardless of whether the solubilizing substituent was attached at the A or B position on the benzimidazole ring.

The trimethyl-lock (TML) prodrug strategy has been extensively explored as an effective method for increasing solubility and enhancing delivery of a wide variety of drug molecules.[27] Following dephosphorylation, a rapid lactonization of the ortho-hydroxyphenyl-

dimethylpropionate promoiety results in efficient drug release.[22] TML prodrug **9** provided high plasma concentrations of PIB in mouse and dog; 4-fold higher in mouse in comparison to dosing with PIB alone. Prodrug **9** had excellent hydrolytic stability, with no significant degradation observed after 24 hours at 37 $^{o}$C in neutral pH buffer, making it one of the most stable ester-linked prodrugs that we investigated. Solubility of **9** in neutral phosphate buffer was low, but measurable (unlike PIB which has no measurable solubility above pH 2). The good solubility in FESSIF for **9** would indicate adequate dissolution in the GI, which is consistent with the excellent PK performance of this prodrug.

Prodrugs were selected for PK studies in monkey based on overall properties of solubility and stability, as well as the ability to efficiently deliver PIB in PK studies in mouse and dog. Select prodrugs were dosed as a suspension in 0.5% HPMC (dose adjusted for MW of the prodrug to deliver 2 mg/kg PIB equivalent), and multiple plasma samples were collected at regular time intervals up to 12 hours post dosing to determine concentrations of both PIB and the prodrug that was dosed. Prodrugs were not detected in any of the plasma samples, with the exception of prodrug **2**, which was present in low concentrations in samples collected up to 6 hours post dosing (AUC PIB/AUC **2** = 40). Several prodrugs tested in monkey provided equal or better AUC/dose in comparison to dosing with PIB (Figure 3), including phosphomethyl prodrug **2**, valine ester prodrug **14**, phosphophenylacetate prodrugs **6** and **25**, and trimethyl-lock prodrug **9**. Disappointing results for pyridylcarbamate prodrug **28** were confirmed in a repeat study. The most likely explanation for the poor performance of prodrugs **26** and **28** is inefficient drug release by intestinal ALP in monkey, but we have no evidence to support this theory and PK studies in monkey with similar prodrugs have not been reported.

Of the phosphate prodrugs that performed well in monkey, **2**, **6**, and **9** were selected as the most promising prospects for development based on an overall profile of improved solubility relative to PIB, hydrolytic stability properties deemed adequate to initiate salt-selection studies (half-life > 24 h in stability assays), and efficient delivery of PIB in PK studies in multiple preclinical species (Table 3).

Figure 3. Monkey PK for PIB prodrugs.

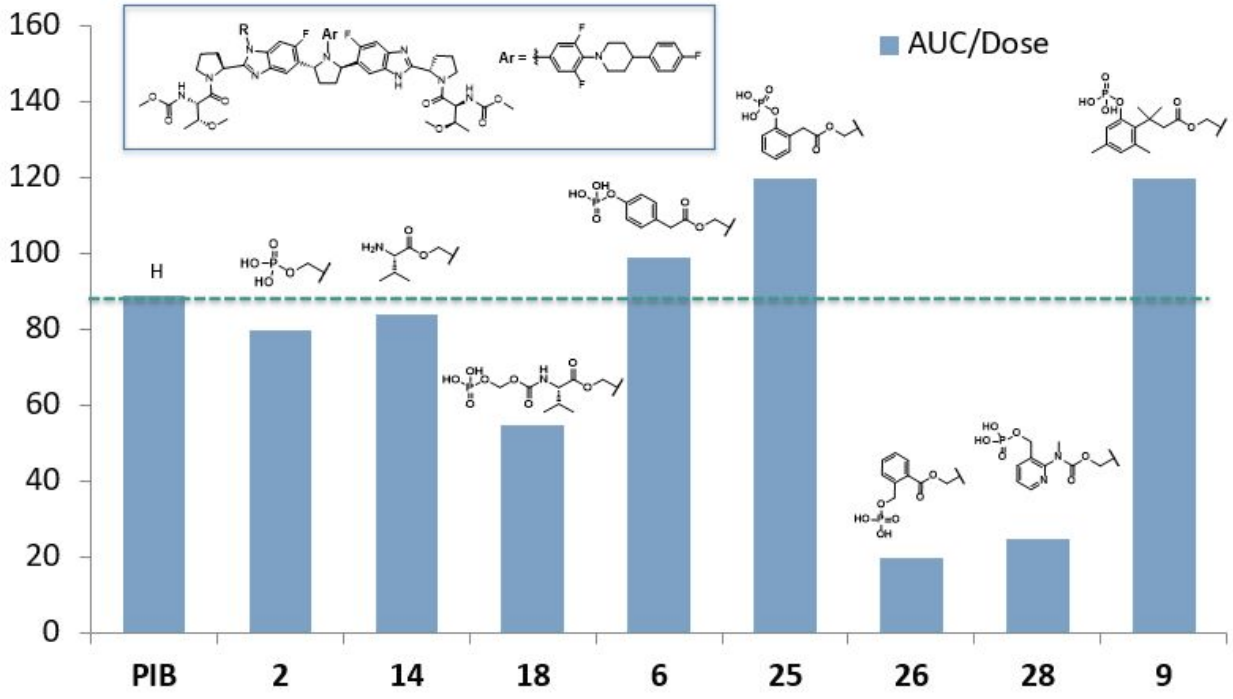


Table 3. Properties of leading PIB prodrug development candidates.

| Property | PIB | 2 | 6 | 9 |
|---|---|---|---|---|
| **Aq. Sol. mg/mL (pH 7.4)** | < 0.1 | 6.5 [>65x PIB] | 135 | 0.5 [>5x PIB] |
| **Calc. LogD (pH 7.4)** | 7.6 | 3.8 | 5.5 | 7.5 |
| **FeSSIF Sol. μg/mL (pH 5)** | 169 | -- | >1000 | 794 [5x PIB] |
| **Stability ($t_{1/2}$ @ pH 7.4)** | -- | > 3 days | > 1 day | > 3 days |
| **Mouse AUC (ng·h/mL) PIB equiv. dose = 6 mg/kg** | 6,720 | 2,660* | 16,100 | 20,600 |
| **Dog AUC (ng·h/mL) PIB equiv. dose = 40 mg** | 3,860 | 429 | 1,920 | 3,210 |
| **Monkey AUC (ng·h/mL) PIB equiv. dose = 2 mg/kg** | 166 | 160 | 197 | 240 |

*dosed at 3 mg/kg PIB equiv. dose

## Conclusion

A research program to identify solubilizing prodrugs of PIB identified three phosphate analogs, each having important differences in properties as determined by their promoiety

linking group. Not surprisingly, hydrolytic stability favored non-ester containing phosphomethyl prodrug **2**, while prodrug efficiency determined by performance in PK studies favored the ester-linked prodrugs, particularly TML prodrug **9**. The relative PK performance, which was not related to observed solubility differences, was likely due to the drug releasing efficiency of the promoiety group. Differences in the rate of dephosphorylation by intestinal alkaline phosphatase may account for the relative performance of prodrugs **2** and **9**, while prodrug **6** required esterase activity to release the drug.[28] The observed differences in solubility for PIB phosphate prodrugs are not well understood. Properties of the promoiety matter, as evidenced by the poor solubility of the highly lipophilic TML prodrug **9**, which has a calculated LogD very similar to PIB. Phosphate solubilization for these prodrugs may be affected by overall conformation in solution, which could be an explanation for the solubility differences observed for isomeric prodrugs having substituents in positions A or B of the benzimidazole. Solid forms of all prodrugs evaluated were amorphous, consistent with chromatographic isolation. However, obtaining a crystalline solid form is necessary to assess stability and hygroscopicity prior to initiating formulation studies. The three prodrugs identified were advanced to salt selection experiments, with the goal of identifying a crystalline solid form. Hydrolytic stability for prodrug **6** was not adequate to obtain a stable salt form, prohibiting its advancement. Stable salt forms of **2** and **9** were identified and are being investigated.

PIB presented unique challenges to the identification of solution-stable prodrugs with improved aqueous solubility. Nitrogen atoms on the two unsymmetrically substituted benzimidazole groups provided the only convenient handle for installing the solubilizing group, giving rise to a difficult regioselectivity problem for synthesis. Promoiety designs that provided suitable stability and good drug-releasing properties focused largely on the oxymethyl ester linking strategy, however a convenient synthetic method using chloromethyl ester alkylating reagents was selective for forming the regioisomer that was less desirable from a solubility perspective. It is possible that the lessons learned in our work to identify solubilizing prodrugs of PIB may be applicable to the unique structural features of this drug and might not inform prodrug studies with other drug molecules. Nevertheless, strategies implemented here may

provide a useful guide for approaches worth considering with other large and lipophilic compounds where solubility-limited exposure prohibits advancement or requires over-extensive enabling formulation technology.

## Experimental

**General Procedures.** Reagents and solvents, including anhydrous solvents, were obtained from commercial sources and used as supplied. Column chomatography was carried out on silica gel. $^{1}$H NMR spectra were measured using a Varian 400-MR (400 MHz) or a Varian Inova 500 (500 MHz) spectrometer. Chemical shifts are reported in ppm (δ) and referenced to an internal standard of tetramethylsilane (δ 0.00 ppm). $^{1}$H – $^{1}$H couplings are assumed to be first-order, and peak multiplicities are reported in the usual manner. MS analysis was conducted using a Finnigan SSQ7000 (ESI) mass spectrometer. Prodrugs were determined to be >95% pure by analytical HPLC using an Agilent 1260 LC System (HPLC conditions: Agilent poroshell 120 EC-C18 2.7 um, 4.6 x 150 mm; 5 uL injection, 1.0 mL/min flow rate, 25 $^{o}$C column; A: 0.1% H3PO4; B: ACN; 5% B for 1 min, ramp to 100% B at 18 min, hold 1 min).

**Methods used to determine solubility of compounds.** For equilibrium solubility, sufficient solid was added to 3–4 mL liquid medium in triplicate such that excess solid remained undissolved. The mixtures were equilibrated for 24–48 hours at 25 rpm on an end-over-end tumbler model in a constant temperature water bath (25 ºC). After equilibration, the mixtures were inspected to assure that excess solid remained. If not, additional solid was added, and the mixtures were again equilibrated for 24–48 hours. The pH of aqueous suspensions was determined after equilibration. The solid phase was separated from the liquid phase by centrifugation at 4000 rpm at equilibration temperature 25 ºC. The supernatant was then filtered through a 0.45 µm GHP membrane filter to discard the initial 2 mL (to saturate filter) and capture the last 1 mL for analysis. The filtrate was diluted as needed for quantification and injected to HPLC. The concentration was evaluated by linear regression against known concentration standards.

**Methods used to determine hydrolytic stability of compounds.** A stock solution of prodrug was prepared in DMSO (~1.25mg/mL). This DMSO stock was diluted into 0.1N HCl (pH 1) and 50 mM phosphate buffer (pH 7.4) for a final prodrug concentration of ~125ug/mL and DMSO concentration of 10%. The solution was filtered through a 0.45 µm GHP membrane filter and placed into an HPLC vial. The vial was inserted into a heated HPLC autosampler (37 $^{o}$C) and

injections were made at multiple time points over the course of 24hrs. Percent recovery based on prodrug peak area was calculated relative to the time 0 injection.

**Methods for Pharmacokinetic evaluation of compounds.** CD-1 mice were obtained from Charles River Laboratories (Wilmington, MA). Beagle dogs (male/female) were obtained from Marshall Farms (North Rose, NY). Cynomolgus monkeys (female) were obtained from Covance (Denver, PA). Mice were allowed free access to food and water; dogs and monkeys were fasted overnight prior to dosing with free access to water. Food was returned to dogs 12 hours after dosing or 4 hours after drug administration in monkeys. Compounds were dosed as follows: in mouse by oral gavage as a solution or suspension in 0.2% HPMC at 10 mL/kg; in dog in a gelatin capsule as a solution or suspension in 0.2% HPMC at 0.5 mL/kg; in monkey by gastric intubation as a solution or suspension in 0.5% HPMC at 0.5 mL/kg. Blood samples, collected into $K_2$EDTA anticoagulant for plasma concentration analysis, were obtained from each animal after dosing. Serial samples were obtained at 0.25, 0.5, 1.0, 3, 6, 9, 12 and 24 hours post dosing in mice and at 0.25, 0.5, 1.0, 1.5, 2, 3, 4, 6, 9, 12 and 24 hours post dosing in dogs and monkeys. Plasma was separated by centrifugation (3200 x g, 5 minutes, ~4°C) and stored frozen (<-15°C) until analysis.

All animal studies were approved by the AbbVie Institutional Animal Care and Use Committee (IACUC) and conducted in an AAALAC accredited facility to ensure high standards of animal care and use.

**Methyl ((2*S*,3*R*)-1-((*S*)-2-(6-((2*R*,5*R*)-1-(3,5-difluoro-4-(4-(4-fluorophenyl)piperidin-1-yl)phenyl)-5-(5-fluoro-2-((*S*)-1-(N-(methoxycarbonyl)-*O*-methyl-L-threonyl)pyrrolidin-2-yl)-1*H*-benzo[d]imidazol-6-yl)pyrrolidin-2-yl)-5-fluoro-1-((phosphonooxy)methyl)-1*H*-benzo[d]imidazol-2-yl)pyrrolidin-1-yl)-3-methoxy-1-oxobutan-2-yl)carbamate (1).** To a solution of dimethyl ((2*S*,2'*S*,3*R*,3'*R*)-((2*S*,2'*S*)-2,2'-(6,6'-((2*R*,5*R*)-1-(3,5-difluoro-4-(4-(4-fluorophenyl)piperidin-1-yl)phenyl)pyrrolidine-2,5-diyl)bis(5-fluoro-1*H*-benzo[d]imidazole-6,2-diyl))bis(pyrrolidine-2,1-diyl))bis(3-methoxy-1-oxobutane-2,1-diyl))dicarbamate (PIB, 1.0 g, 0.90 mmol) in anhydrous *N,N*-dimethylformamide at 0 °C was added sodium hydride (60% suspension in mineral oil, 54 mg, 1.35 mmol), and the resulting mixture was stirred at 0°C for 30 minutes. Di-tert-butyl (chloromethyl) phosphate (0.23 g, 0.90 mmol) was added, and the

mixture was allowed to warm to ambient temperature and stirred for 16 hours. The mixture was partitioned between 0.5 N aqueous HCl and ethyl acetate, and the organic layer was dried over $Na_2SO_4$, filtered and concentrated in vacu. The crude product was dissolved in dichloromethane (10 mL), and the solution was cooled in an ice bath while trifluoroacetic acid (3 mL) was added dropwise. The resulting solution was allowed to warm to ambient temperature and stirred for 3 hours. The solution was concentrated in vacuo, and the crude product mixture was purified by C18 HPLC using a solvent gradient of 5-100% acetonitrile in 0.1% TFA aqueous buffer. Bis-phosphomethyl products eluted at 40-50% acetonitrile, followed by **1**, which was the first mono-alkyl product to elute. Lyophilization provided **1** as a colorless solid (0.22 g, 0.18 mmol, 20% yield): $^1$H NMR (400 MHz, DMSO-$d_6$) δ 7.58 (d, *J* = 10.2 Hz, 1H), 7.51 – 7.40 (m, 2H), 7.28 – 6.98 (m, 6H), 6.15 – 5.99 (m, 2H), 5.91 – 5.82 (m, 2H), 5.66 (d, *J* = 7.9 Hz, 1H), 5.55 (d, *J* = 8.3 Hz, 1H), 5.31 (dd, *J* = 7.3, 4.9 Hz, 1H), 5.13 (dd, *J* = 8.1, 4.8 Hz, 1H), 4.28 – 4.20 (m, 2H), 3.97 – 3.75 (m, 4H), 3.51 (s, 3H), 3.50 (s, 3H), 3.37 – 2.82 (m, 10H), 2.75 – 1.49 (m, 21H), 1.05 – 0.88 (m, 6H); MS (ESI) *m/z* 1223.3 $[M+H]^+$.

**Methyl ((2*S*,3*R*)-1-((*S*)-2-(5-((2*R*,5*R*)-1-(3,5-difluoro-4-(4-(4-fluorophenyl)piperidin-1-yl)phenyl)-5-(5-fluoro-2-((*S*)-1-(N-(methoxycarbonyl)-*O*-methyl-L-threonyl)pyrrolidin-2-yl)-1*H*-benzo[d]imidazol-6-yl)pyrrolidin-2-yl)-6-fluoro-1-((phosphonooxy)methyl)-1*H*-benzo[d]imidazol-2-yl)pyrrolidin-1-yl)-3-methoxy-1-oxobutan-2-yl)carbamate (2).** Compound **2** was prepared using the methods described for synthesis of **1**. It was the second of 2 mono-alkylated products to elute during the HPLC purification step, and was obtained as a colorless solid by lyophilization (0.16 g, 0.13 mmol, 14% yield): $^1$H NMR (501 MHz, DMSO-$d_6$) δ 7.67 – 7.53 (m, 2H), 7.28 – 6.96 (m, 7H), 6.25 (t, *J* = 10.7 Hz, 1H), 6.02 (t, *J* = 11.0 Hz, 1H), 5.91 – 5.81 (m, 2H), 5.67 – 5.53 (m, 2H), 5.34 – 5.28 (m, 1H), 5.14 (dd, *J* = 8.2, 4.8 Hz, 1H), 4.26 (dd, *J* = 8.3, 6.1 Hz, 1H), 4.18 (dd, *J* = 8.2, 5.9 Hz, 1H), 3.88 – 3.70 (m, 4H), 3.52 (s, 3H), 3.50 (s, 3H), 3.34 – 2.79 (m, 10H), 2.71 – 1.52 (m, 21H), 1.08 – 0.69 (m, 6H); MS (ESI) *m/z* 1223.2 $[M+H]^+$.

**Methyl 2-(4-((di-*tert*-butoxyphosphoryl)oxy)phenyl)acetate (30).** To a stirring solution of methyl 2-(4-hydroxyphenyl)acetate (2.49 g, 15.0 mmol) and 1*H*-tetrazole (83 mL, 37.5 mmol) in *N,N*-dimethylacetamide (30.0 mL) was added di-*tert*-butyl diisopropylphosphoramidite (5.92 ml, 18.8 mmol), and the resulting mixture was stirred at ambient temperature for 4 hours. The

mixture was then cooled to 0 °C, a solution of 50% aqueous hydrogen peroxide (2.30 ml, 37 mmol) was added, and the mixture was allowed to warm to ambient temperature and stirred for 2 hours. The mixture was partitioned between saturated aqueous $Na_2CO_3$ and ethyl acetate (3x), and the combined organic layers were dried over $Na_2SO_4$, filtered, and concentrated in vacuo. The crude product was purified by column chromatography on silica gel, eluting with a solvent gradient of 0-100% ethyl acetate in heptanes. Compound **30** was obtained as a colorless oil (5.2 g, 97%): $^1$H NMR (501 MHz, DMSO-$d_6$) δ 7.31 – 7.22 (m, 4H), 7.15 – 7.06 (m, 2H), 3.66 (s, 2H), 3.61 (s, 3H), 1.44 (s, 18H).

**Chloromethyl 2-(4-((di-*tert*-butoxyphosphoryl)oxy)phenyl)acetate (5).** A solution of **30** (5.2 g, 14.51 mmol) in water (60.5 mL) and tetrahydrofuran (151 mL) was cooled to 0 °C, and a solution of aqueous lithium hydroxide (0.3 M, 145 mL, 43.5 mmol) was added dropwise. The reaction was stirred at 0 °C for 60 min, and 1.0 M aqueous HCl was added to acidify to pH 3.0. The mixture was extracted with ethyl acetate, and the organic layer was washed with water and brine. The solution was dried over $Na_2SO_4$, filtered, and concentrated in vacuo to give a colorless oil, which was dissolved in dichloromethane (24 mL). To the solution was added water (24 mL), $NaHCO_3$ (4.78 g, 56.9 mmol) and tetrabutylammonium hydrogen sulfate (0.48 g, 1.42 mmol), and the resulting mixture was cooled to 0 °C and vigorously stirred while chloromethyl chlorosulfate (2.59 ml, 28.5 mmol) was added dropwise. The stirred reaction mixture was allowed to slowly warm to ambient temperature over 3 hours. The layers were separated, and the organic layer was dried over $Na_2SO_4$, filtered, and concentrated in vacuo. The crude product was purified by column chromatography on silica gel using a solvent gradient of 0-100% ethyl acetate in heptanes. Compound **5** was obtained as a colorless oil (2.53 g, 6.44 mmol, 45% yield): $^1$H NMR (400 MHz, $CDCL_3$) δ 7.25 – 7.16 (m, 4H), 5.70 (s, 2H), 3.66 (s, 2H), 1.51 (s, 18H).

***Tert*-butyl 6-((2*R*,5*R*)-1-(3,5-difluoro-4-(4-(4-fluorophenyl)piperidin-1-yl)phenyl)-5-(6-fluoro-2-((*S*)-1-((2*S*,3*R*)-3-methoxy-2-((methoxycarbonyl)amino)butanoyl)pyrrolidin-2-yl)-1*H*-benzo[d]imidazol-5-yl)pyrrolidin-2-yl)-5-fluoro-2-((*S*)-1-((2*S*,3*R*)-3-methoxy-2-((methoxycarbonyl)amino)butanoyl)pyrrolidin-2-yl)-1*H*-benzo[d]imidazole-1-carboxylate (3).** To a stirred solution of dimethyl ((2S,2'S,3R,3'R)-((2S,2'S)-2,2'-(5,5'-((2R,5R)-1-(3,5-difluoro-4-(4-

(4-fluorophenyl)piperidin-1-yl)phenyl)pyrrolidine-2,5-diyl)bis(6-fluoro-1H-benzo[d]imidazole-5,2-diyl))bis(pyrrolidine-2,1-diyl))bis(3-methoxy-1-oxobutane-2,1-diyl))dicarbamate (PIB, 14.8 g, 13.3 mmol) in anhydrous tetrahydrofuran (111 mL) was added a solution of di-*tert*-butyl dicarbonate (2.18 g, 10.0 mmol) and 4-dimethylaminopyridine (0.12 g, 1.0 mmol) in anhydrous tetrahydrofuran (111 mL), dropwise over 60 minutes. The reaction mixture was poured into water (250 mL) and extracted with ethyl acetate (2 x 200 mL), and the combined organic layers were washed with brine, dried over $Na_2SO_4$, filtered, and concentrated in vacuo. The crude product was purified by column chromatography on silica gel, eluting with a solvent gradient of 0-10% methanol in ethyl acetate. Compound **3**, which is a mixture of mono-Boc benzimidazole regioisomers, was obtained as an off-white solid (6.49 g, 54% yield).

**(5-((2*R*,5*R*)-1-(3,5-Difluoro-4-(4-(4-fluorophenyl)piperidin-1-yl)phenyl)-5-(5-fluoro-2-((*S*)-1-((2*S*,3*R*)-3-methoxy-2-((methoxycarbonyl)amino)butanoyl)pyrrolidin-2-yl)-1*H*-benzo[d]imidazol-6-yl)pyrrolidin-2-yl)-6-fluoro-2-((*S*)-1-((2*S*,3*R*)-3-methoxy-2-((methoxycarbonyl)amino)butanoyl)pyrrolidin-2-yl)-1*H*-benzo[d]imidazol-1-yl)methyl 2-(4-(phosphonooxy)phenyl)acetate (6).** To a solution of **3** (2.0 g, 1.65 mmol) in anhydrous *N,N*-dimethylformamide (16.5 mL) was added cesium carbonate (0.81 g, 2.47 mmol), and the resulting mixture was stirred at ambient temperature for 10 minutes. Compound **5** (1.30 g, 3.30 mmol) was added, and the reaction mixture was stirred at ambient temperature for 90 minutes. The reaction was quenched by the addition of saturated aqueous $NH_4Cl$, and the mixture was extracted with methyl *tert*-butyl ether (3 x 100 ml). The combined organic layers were washed with water (2 x 100 mL) and brine, dried over $Na_2SO_4$, filtered, and concentrated in vacuo. The crude product was purified by column chromatography on silica gel using a solvent gradient of 50-100% ethyl acetate in heptanes to give a mixture of mono-alkylated benzimidazole regioisomeric products as a colorless solid (1.34 g, 51%). A portion of this solid (0.35 g, 0.22 mmol) was dissolved in dichloromethane (3.72 mL) and the solution was cooled to 0 °C. Trifluoroacetic acid (0.74 mL) was added, and the solution was allowed to warm to ambient temperature and stirred for 1 hour. The solution was concentrated in vacuo, and the residue was dissolved in dichloromethane (5 ml) and concentrated in vacuo (2x). The crude product was purified by C18 preparative HPLC, eluting with a solvent gradient of 20-95%

acetonitrile in 0.1% aqueous TFA buffer. Compound **6** was isolated as a colorless solid by lyophilization (0.18 g, 0.13 mmol, 60% yield): $^1$H NMR (400 MHz, DMSO-$d_6$) δ 7.67 (t, *J* = 10.1 Hz, 2H), 7.33 – 7.20 (m, 5H), 7.16 (d, *J* = 6.8 Hz, 1H), 7.14 – 7.04 (m, 5H), 6.99 (d, *J* = 8.3 Hz, 1H), 6.39 (s, 2H), 5.91 (s, 1H), 5.88 (s, 1H), 5.70 – 5.64 (m, 1H), 5.58 (d, *J* = 6.1 Hz, 1H), 5.24 (dd, *J* = 7.6, 4.4 Hz, 1H), 5.18 (dd, *J* = 8.2, 5.1 Hz, 1H), 4.28 (dd, *J* = 8.5, 5.8 Hz, 5H), 4.20 (dd, *J* = 8.2, 6.0 Hz, 2H), 3.83 (m, 4H), 3.73 (m, 2H), 3.52 (d, *J* = 8.0 Hz, 6H), 3.42 – 3.37 (m, 1H), 3.32 (p, *J* = 5.7 Hz, 2H), 3.07 – 2.93 (m, 6H), 2.87 (m, 4H), 2.56 (m, 1H), 2.47 (m, 2H), 2.39 – 1.93 (m, 6H), 1.83 (d, *J* = 9.6 Hz, 2H), 1.74 – 1.57 (m, 4H), 0.95 (d, *J* = 6.2 Hz, 3H), 0.77 (d, *J* = 6.2 Hz, 3H); MS (ESI) *m/z* 1357.3 $[M+H]^+$.

**Chloromethyl 3-(2-((bis(benzyloxy)phosphoryl)oxy)-4,6-dimethylphenyl)-3-methylbutanoate (8).** A solution of 3-(2-((bis(benzyloxy)phosphoryl)oxy)-4,6-dimethylphenyl)-3-methylbutanoic acid (**7**, 2.05 g, 4.25 mmol), prepared according to reference 22, in dichloromethane (20 mL) was stirred at ambient temperature. Sodium bicarbonate (1.43 g, 16.99 mmol), tetrabutylammonium hydrogen sulfate (0.14 g, 0.43 mmol), and water (20 mL) were added. Chloromethyl chlorosulfate (0.513 ml, 5.10 mmol) was added dropwise, and the mixture was heated to 30-35 °C. After 15 minutes, the layers were separated, and the organic layer was dried over $Na_2SO_4$, filtered, and concentrated in vacuo. The crude product was purified by column chromatography on silica gel using a solvent gradient of 20-60% methyl *tert*-butyl ether in heptanes. Compound **8** was obtained as an oil (2.02 g, 3.80 mmol, 90 % yield): $^1$H NMR (501 MHz, $CDCl_3$) δ 7.36 – 7.27 (m, 10H), 7.09 (brs, 1H), 6.72 (brs, 1H), 5.45 (s, 2H), 5.15 – 5.07 (m, 4H), 2.95 (s, 2H), 2.52 (s, 3H), 2.16 (s, 3H), 1.58 (s, 6H).

**(5-((2R,5R)-1-(3,5-Difluoro-4-(4-(4-fluorophenyl)piperidin-1-yl)phenyl)-5-(6-fluoro-2-((*S*)-1-((2*S*,3*R*)-3-methoxy-2-((methoxycarbonyl)amino)butanoyl)pyrrolidin-2-yl)-1*H*-benzo[d]imidazol-5-yl)pyrrolidin-2-yl)-6-fluoro-2-((*S*)-1-((2*S*,3*R*)-3-methoxy-2-((methoxycarbonyl)amino)butanoyl)pyrrolidin-2-yl)-1*H*-benzo[d]imidazol-1-yl)methyl 3-(2-((bis(benzyloxy)phosphoryl)oxy)-4,6-dimethylphenyl)-3-methylbutanoate (31).** A solution of dimethyl ((2*S*,2'*S*,3*R*,3'*R*)-((2*S*,2'*S*)-2,2'-(5,5'-((2*R*,5*R*)-1-(3,5-difluoro-4-(4-(4-fluorophenyl)piperidin-1-yl)phenyl)pyrrolidine-2,5-diyl)bis(6-fluoro-1*H*-benzo[d]imidazole-5,2-diyl))bis(pyrrolidine-2,1-diyl))bis(3-methoxy-1-oxobutane-2,1-diyl))dicarbamate (PIB, 8.43 g,

7.57 mmol) in anhydrous *N,N*-dimethylformamide (42 mL) was cooled to 10 °C and potassium *tert*-butoxide (1 M in tetrahydrofuran, 6.81 mL, 6.81 mmol) was added dropwise. After 5 minutes with cooling to 5 °C, a solution of **8** (2.01 g, 3.79 mmol) in *N,N*-dimethylformamide (1 ml) was added, and the mixture was allowed to warm to ambient temperature and stirred for 14 hours. To the reaction mixture was added aqueous 1 N HCl (45 mL) and ethyl acetate (90 mL), and the mixture was stirred for 15 min. The layers were separated, and the aqueous layer was extracted with ethyl acetate (45 mL). The combined organic layers were washed with aqueous 1N HCl (18 mL), brine (18 mL), saturated aqueous $NaHCO_3$ (18 mL), and brine (18 mL). The organic layer was dried over $Na_2SO_4$, filtered and concentrated, and the crude product was purified by column chromatography on silica gel using a solvent gradient of 50-100% 19:1 ethyl acetate:isopropanol in heptanes. Compound **31** was obtained as a colorless foam (2.37 g, 1.47 mmol, 39 % yield): $^1$H NMR (501 MHz, DMSO-$d_6$) δ 7.43 – 7.02 (m, 19H), 6.94 (br s, 1H), 6.78 (brs, 1H), 6.44 (br s, 1H), 6.30 (d, *J* = 11.7 Hz, 1H), 6.14 (d, *J* = 11.7 Hz, 1H), 5.84 (br s, 2H), 5.65-5.45 (m, 2H), 5.18-5.09 (m, 2H), 5.06 (s, 2H), 5.05 (s, 2H), 4.26 (br s, 1H), 4.17 (t, *J* = 7.2 Hz, 1H), 3.81 (br s, 2 H), 3.74-3.65 (m, 1H), 2.81 (s, 3H), 3.51 (s, 3H), 3.52-2.77 (m, 18H), 2.57-2.32 (m, 5H), 2.25 (s, 3H), 2.03 (s, 3H), 1.47 (s, 3H), 1.44 (s, 3H), 2.27-1.38 (m, 9H), 1.08-0.88 (m, 4H), 0.73 (d, 3H); MS (ESI) *m/z* 1608 $[M+H]^+$.

**(5-((2*R*,5*R*)-1-(3,5-difluoro-4-(4-(4-fluorophenyl)piperidin-1-yl)phenyl)-5-(6-fluoro-2-((S)-1-((2S,3R)-3-methoxy-2-((methoxycarbonyl)amino)butanoyl)pyrrolidin-2-yl)-1H-benzo[d]imidazol-5-yl)pyrrolidin-2-yl)-6-fluoro-2-((S)-1-((2S,3R)-3-methoxy-2-((methoxycarbonyl)amino)butanoyl)pyrrolidin-2-yl)-1H-benzo[d]imidazol-1-yl)methyl 3-(2,4-dimethyl-6-(phosphonooxy)phenyl)-3-methylbutanoate (9).** To a solution of **31** (1.59 g, 0.99 mmol) in tetrahydrofuran (11 mL) was added to 20% $Pd(OH)_2$/C, wet (163 mg, 0.59 mmol) in a 25 ml SS reactor. The reactor was purged with argon and the mixture was stirred under 50 psi of hydrogen at 25 °C. After 16 hours, the mixture was filtered through a Celite packed column and the catalyst was washed thoroughly with methanol. Acetonitrile (80 mL) was added, and the mixture was sonicated and then stirred vigorously for 10 minutes to give the crude product as a colorless solid. The crude product was purified by C18 preparative HPLC using a solvent gradient of 40-95% acetonitrile in 0.1% aqueous TFA buffer. The clean fractions were pooled

and concentrated in vacuo to ~10 mL to give a colorless slurry. The solid product was collected by filtration, washed with water, and dried under vacuum to give **9** as a colorless solid (0.86 g, 0.60 mmol, 61% yield): $^1$H NMR (400 MHz, DMSO-$d_6$) δ 7.39 (dd, *J* = 10.7, 7.8 Hz, 2H), 7.22 (dd, *J* = 8.7, 5.5 Hz, 2H), 7.10 (dd, *J* = 7.2, 3.4 Hz, 2H), 7.03 (t, *J* = 8.8 Hz, 2H), 6.95 (s, 1H), 6.92 (d, *J* = 8.8 Hz, 1H), 6.29 (s, 1H), 6.25 (d, *J* = 11.6 Hz, 1H), 6.13 (d, *J* = 11.8 Hz, 1H), 5.82 (brd, *J* = 13.0 Hz, 2H), 5.55 (dd, *J* = 20.7, 6.0 Hz, 2H), 5.11 (ddd, *J* = 18.6, 7.6, 4.4 Hz, 2H), 4.22 (t, *J* = 7.4 Hz, 1H), 4.14 (dd, *J* = 8.3, 5.8 Hz, 1H), 3.85-2.73 (m, 21H), 3.04 (s, 3H), 2.94 (s, 2H), 2.79 (s, 2H), 2.31-1.69 (m, 10H), 2.18 (s, 4H), 2.05 (s, 3H), 1.69-1.50 (m, 4H), 1.46 (s, 3H), 1.42 (s, 3H), 1.04-0.89 (m, 3H), 0.70 (d, *J* = 6.2 Hz, 3H); MS (ESI) *m/z* 1428 $[M+H]^+$.

## ASSOCIATED CONTENT

Supporting Information

Synthetic methods and analytical data for compounds **10**, **11**, **12, 13, 14, 15, 16, 17, 18, 19, 20, 21, 22, 23, 24, 25, 26, 27, 28, 29**; analytical HPLC for **2**, **6**, and **9**; molecular formula strings. This material is available free of charge via the Internet at http://pubs.acs.org.

## AUTHOR INFORMATION

**Corresponding Author**

*John T. Randolph - Phone: +1 847-937-7182. E-mail: john.randolph@abbvie.com.

## ABBREVIATIONS USED:

HCV, hepatitis C virus; PIB, pibrentasvir; GLE, glecaprevir; GT, genotype; DAA, direct-acting antiviral; SVR, sustained virologic response; NS, nonstructural; FESSIF, fed-state simulated intestinal fluid; PK, pharmacokinetics; PAMPA, parallel artificial membrane permeability assay; MDCK, Madin-Darby canine kidney, TFA, trifluoroacetic acid; DMF, *N,N*-dimethylformamide; DMAP, 4-dimethylaminopyridine; Boc, *tert*-butoxy carbonyl.

**Disclosure:** All authors are employees of AbbVie. The design, study conduct, and financial support for this research were provided by AbbVie and Enanta. AbbVie and Enanta participated in the interpretation of data, review, and approval of the publication.

**References**

1. Lamb, Y. N. Glecaprevir/Pibrentasvir: First Global Approval *Drugs* **2017**, *77*, 1797-1804.

2. Forns, X.; Lee, S. S.; Valdes J.; Lens, S.; Ghalib, R.; Aguilar, H.; Felizarta, F.; Hassanein, T.; Hinrichsen, H.; Rincon, D.; Morillas, R.; Zeuzem, S.; Horsmans, Y.; Nelson, D. R.; Yu, Y.; Krishnan, P.; Lin C.-W.; Kort, J. J.; Mensa, F. J. Glecaprevir Plus pibrentasvir for Chronic Hepatitis C Virus Genotype 1, 2, 4, 5, or 6 Infection in Adults with Compensated Cirrhosis (EXPEDITION-1): A Single-Arm, Open-Label, Multicenter Phase 3 Trial *Lancet* **2017**, *17*, 1062-1068.

3. Puoti, M.; Foster, G. R.; Wang, S.; Mutimer, D.; Gane, E.; Moreno, C.; Chang, T. T.; Lee, S. S.; Marinho, R.; Dufour, J.-F.; Pol, S.; Hezode, C.; Gordon, S. C.; Strasser, S. I.; Thuluvath, R. J.; Zhang, Z.; Lovell, S.; Pilot-Matias, T.; Mensa, F. J. High SVR12 with 8-Week and 12-Week Glecaprevir/Pibrentasvir Therapy: An Integrated Analysis of HCV Genotype 1-6 Patients without Cirrhosis *J Hepatol.* **2018**, *69*, 293-300.

4. Brown, R. S. Jr; Buti, M.; Rodrigues, L.; Chulanov, V.; Chuang, W.-L.; Aguilar, H.; Horvath, G.; Zuckerman, E.; Carrion, B. R.; Rodriguez-Perez, F.; Urbanek, P.; Abergel, A.; Cohen, E.; Lovell, S. S.; Schnell, G.; Lin, C.-W.; Zha, J.; Wang, S.; Trinh, R.; Mensa, F. J.; Burroughs, M.; Felizarta, F. Glecaprevir/Pibrentasvir for 8 Weeks in Treatment-Naïve Patients with Chronic HCV Genotypes 1-6 and Compensated Cirrhosis: The EXPEDITION-8 Trial *J. Hepatol.* **2020**, *72*, 441-449.

5. Mensa, F. J.; Lovell, S.; Pilot-Matias, T.; Liu, W. Glecaprevir/Pibrentasvir for the Treatment of Chronic Hepatitis C Virus Infection *Future Microbiol.* **2018**, *14*, 89-110.

6. Huff, J.; Andersen, R. Glecaprevir/Pibrentasvir: The First 8-Week Pangenotypic HCV Treatment Regimen for Patients 12 Years of Age and Older *Annals of Pharmacother.* **2020**, *54*, 262-276.

7. Wagner, R.; Randolph, J. T.; Patel, S. V.; Nelson, L.; Matulenko, M. A.; Keddy, R.; Pratt, J. K.; Liu, D.; Krueger, A. C.; Donner, P. L.; Hutchinson, D.; Flentge, C.; Betebenner, D.; Rockway, T.; Maring, C. J.; Ng, T.; Krishnan, P.; Pilot-Matias, T.; Panchel, N.; Reisch, T.; Dekhtyar, T.; Mondal, R.; Stolarik, D. F.; Gao, Y.; Gao, W.; Beno, D. W. A.; Kati, W. M. Highlights of the Structure-Activity Relationships of Benzimidazole Linked Pyrrolidines Leading to the Discovery of the Hepatitis C Virus NS5A Inhibitor Pibrentasvir (ABT-530) *J. Med. Chem.* **2018**, *61*, 4052-4066.

8. Ng, T. I.; Krishnan, P.; Pilot-Matias, T.; Kati, W.; Schnell, G.; Beyer, J.; Reisch, T.; Lu, L.; Dekhtyar, T.; Irvin, M.; Tripathi, R.; Maring, C.; Randolph, J. T.; Wagner, R.; Collins, C. *In Vitro* Antiviral Activity and Resistance Profile of the Next-Generation Hepatitis C Virus NS5A Inhibitor Pibrentasvir *Antimicrob. Agents Chemother.* **2017**, *61*: e02558-16.

9. Krishnan, P.; Pilot-Matias, T.; Schnell, G.; Tripathi, R.; Ng, T. I.; Reisch, T.; Beyer, J.; Dekhtyar, T.; Irvin, M.; Xie, W.; Larsen, L.; Mensa, F. J.; Collins, C. Pooled Resistance Analysis in HCV Genotype 1-6 Infected Patients Treated with Glecaprevir/Pibrentasvir in Phase 2 and 3 Clinical Trials *Antimicrob Agents Chemother.* **2018**, *62*: e01249-18.

10. Ng, T. I.; Pilot-Matias, T.; Tripathi, R.; Schnell, G.; Krishnan, P.; Reisch, T.; Beyer, J.; Dekhtyar, T.; Irvin, M.; Lu, L.; Asatryan, A.; Campbell, A.; Yao, B.; Lovell, S.; Mensa, F.; Lawitz, E. J.; Kort, J.; Collins, C. Resistance Analysis of a 3-Day Monotherapy Study Glecaprevir or Pibrentasvir in Patients with Chronic Hepatitis C Virus Genotype 1 Infection *Viruses* **2018**, *10*, 462-480.

11. Mavyret dosing guidelines. https://www.rxabbvie.com/pdf/mavyret_pi.pdf (accessed March 17, 2020).

12. Lin, C.-W.; Dutta, S.; Asatryan, A.; Wang, H.; Clifton II, J.; Campbell, A.; Liu, W. Pharmacokinetics, Safety, and Tolerability Following Single and Multiple Doses of Pibrentasvir in a First-in-Human Study *Clin. Pharmacol. Drug Dev.* **2018**, *7*, 44-52.

13. Lin, C.-W.; Dutta, S.; Zhao, W.; Asatryan, A.; Campbell, A.; Liu, W. Pharmacokinetic Interactions and Safety of Coadministration of Glecaprevir and Pibrentasvir in Healthy Volunteers *Eur. J Drug Metab. Pharmacokinet.* **2018**, *43*, 81–90.

14. For a review of properties of large drug molecules, see: Naylor, M. R.; Ly, A. M.; Handford, M. J.; Ramos, D. P.; Pye, C. R.; Furukawa, A.; Klein, V. G.; Noland, R. P.; Edmondson, Q.; Turmon, A. C.; Hewitt, W. M.; Schwochert, J.; Townsend, C. E.; Kelly, C. N.; Blanco, M.-J.; Lokey, R. S. Lipophilic Permeability Efficiency Reconciles the Opposing Roles of Lipophilicity in Membrane Permeability and Aqueous Solubility *J Med. Chem.* **2018**, *61*, 11169-11182.

15. For a review of properties of drug molecules "beyond the rule of 5", see: DeGoey, D. A.; Chen, H.-J.; Cox, P. B.; Wendt, M. D. Beyond the Rule of 5: Lessons Learned from AbbVie's Drugs and Compound Collection *J. Med. Chem.* **2018**, *61*, 2636-2651.

16. For a review of the characteristics of drug target proteins that require large drug molecules for effective therapeutic intervention, see: Doak, B. C.; Zheng, J.; Dobritzsch, D.; Kihlberg, J. How Beyond Rule of 5 Drugs and Clinical Candidates Bind to Their Targets *J. Med. Chem.* **2016**, *59*, 2312-2327.

17. For a recent review on design of solubilizing prodrugs, see: Sanches, B. M. A.; Ferreira, E. I. Bruna M.A. Is Prodrug Design an Approach to Increase Water Solubility? *Internat. J. Pharmaceut.* **2019**, *568*, 118498.

18. Subbaiah, M. A. M.; Meanwell, N. A.; Kadow A. F. Design Strategies in the Prodrugs of HIV-1 Protease Inhibitors to Improve the Pharmaceutical Properties *Eur. J. Med. Chem.* **2017**, *139*, 865-883.

19. Furfine, E. S.; Baker, C. T.; Hale, M. R.; Reynolds, D. J.; Salisbury, J. A.; Searle, A. D.; Studenberg, S. D.; Todd, D.; Tung, R. D.; Spaltenstein, A. Preclinical Pharmacology and Pharmacokinetics of GW433908, a Water-Soluble Prodrug of the Human Immunodeficiency Virus Protease Inhibitor Amprenavir *Antimicrob. Agents Chemother.* **2004**, *48*, 791–798.

20. DeGoey, D. A.; Grampovnik, D. J.; Flosi, W. J.; Marsh, K. C.; Wang, X. C.; Klein, L. L.; McDaniel, K. F.; Liu, Y.; Long, M. A.; Kati, W. M.; Molla, A.; Kempf, D. J. Water-Soluble Prodrugs of the Human Immunodeficiency Virus Protease Inhibitors Lopinavir and Ritonavir *J. Med. Chem.* **2009**, *52*, 2964-2970.

21. Subbaiah, M. A. M.; Mandlekar, S.; Desikan, S.; Ramar, T.; Subramani, L.; Annadurai, M.; Desai, S. D.; Sinha, S.; Jenkins, S. M.; Krystal, M. R.; Subramanian, M.; Sridhar, S.; Padmanabhan, S.; Bhutani, P.; Arla, R.; Singh, S.; Sinha, J.; Thakur, M.; Kadow, J. F.; Meanwell,

N. A. Design, Synthesis, and Pharmacokinetic Evaluation of Phosphate and Amino Acid Ester Prodrugs for Improving the Oral Bioavailability of the HIV-1 Protease Inhibitor Atazanavir *J. Med. Chem.* **2019**, *62*, 3553-3574.

22. Nicolaou, M. G.; Yuan, C.-S.; Borchardt, R. T. Phosphate Prodrugs for Amines Utilizing a Fast Intramolecular Hydroxy Amide Lactonization *J. Org. Chem.* **1996**, *61*, 8636-8641.

23. Lalanne, M.; Andrieux, K.; Couvreur, P. Strategies to Increase the Oral Bioavailability of Nucleoside Analogs *Curr. Med. Chem.* **2009**, *16*, 1391-1399.

24. Krečmerová, M. Amino Acid Ester Prodrugs of Nucleoside and Nucleotide Antivirals *Mini Rev. Med. Chem.* **2017**, *17*, 818-833.

25. Wang, A.; Wu, S.; Tao, Z; Li, X.; Lv, K.; Ma, C.; Li, Y.; Li, L.; Liu, M. Design, Synthesis, and Anti-HBV Activity of New Bis(L-amino acid) Ester Tenofovir Prodrugs *ACS Med. Chem. Lett.* **2019**, *10*, 991-995.

26. Seyedmousavi, S.; Verweij, P. E.; Mouton, J. W. Isavuconazole, a Broad-Spectrum Triazole for the Treatment of Systemic Fungal Diseases *Expert Rev. Anti-Infect. Ther.* **2015**, *13*, 9–27.

27. For a review, see: Levine, M. N.; Raines, R. T. Trimethyl lock: a Trigger for Molecular Release in Chemistry, Biology, and Pharmacology *Chem. Sci.* **2012**, *3*, 2412-2420.

28. Prodrug **6** PK studies included bioanalysis for the hydroxyphenylacetate metabolite, which was not detected at low doses, indicating rapid and efficient esterase-mediated drug release.

Table of contents graphic: